Inorganic Chemistry

Article

pubs.acs.org/IC

Correlations and Differences between Uranium(VI) Arsonates and Phosphonates

Pius O. Adelani,[†] Laurent J. Jouffret,[†] Jennifer E. S. Szymanowski,[†] and Peter C. Burns*[,†,‡]

[†]Department of Civil and Environmental Engineering and Earth Sciences and [‡]Department of Chemistry and Biochemistry, University of Notre Dame, Notre Dame, Indiana 46556, United States

Supporting Information

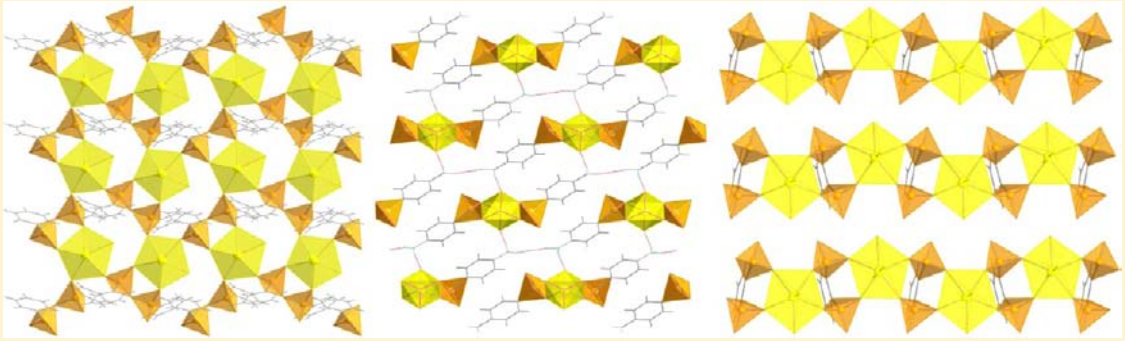

ABSTRACT: Three new uranium arsonate compounds, $UO_2(C_6H_5)_2As_2O_5(H_2O)$ (**UPhAs-1**), $UO_2(HO_3AsC_6H_4AsO_3H)(H_2O)\cdot H_2O$ (**UPhAs-2**), and $UO_2(HO_3AsC_6H_4NH_2)_2\cdot H_2O$ (**UPhAs-3**) have been synthesized under mild hydrothermal conditions. **UPhAs-1** is constructed from UO_7 pentagonal bipyramids that are chelated by the pyroarsonate moiety, $[PhAs(O_2)OAs(O_2)Ph]^{2-}$, forming chains of layered uranyl polyhedra. Two of the phenylarsonic acids are condensed in situ to form the fused tetrahedra of the pyroarsonate moiety through a metal-mediated, thermally induced condensation process. The structure of **UPhAs-2** consists of UO_7 pentagonal bipyramids that are chelated by phenylenediarsonate ligands, forming one-dimensional chains of uranyl polyhedra. **UPhAs-3** consists of a rare UO_6 tetragonally distorted octahedron (D_{4h}) that is on a center of symmetry and linked to two pairs of adjacent 4-aminophenylarsonate ligands. This linear chain structure is networked through hydrogen bonds between the lattice water molecules and the $-NH_2$ moiety. All three of these compounds fluoresce at room temperature, showing characteristic vibronically coupled charge-transfer based emission.

INTRODUCTION

We have had a long-standing interest in the development of uranyl arylphosphonates, mostly because of the major roles they play in nuclear waste management and separation processes.[1] Metal phosphonates have displayed rich and fascinating structural chemistry; most of the structures are layered, and the metal ions are bridged by the phosphonate moiety.[2] The complexities of uranium(VI) phosphonates are illustrated by phase transitions in the uranyl phenylphosphonate system from a cis (α-UPP) to a trans (β-UPP) conformation at room temperature.[3a,b] Upon exposure to an aqueous solution of Na^+ and Ca^{2+} cations, both conformers transformed into a hollow nanotubular form, γ-UPP.[3c] We have also demonstrated that when Rb^+/Cs^+ cations are used to template the structure of uranyl phenyldiphosphonates a remarkable elliptical uranyl nanotubular structure results, $Cs_{3.62}H_{0.38}\{(UO_2)_4[C_6H_4(PO_2OH)_2]_3[C_6H_4(PO_3)_2]F_2\}$.[4a,b] This compound exhibits a high stability and exceptional ion-exchange properties toward monovalent cations. The use of metal and organoammonium cations as structure directing agents has enriched the structural topologies of uranyl arylphosphonates, and the structural complexities have been further enhanced through the design of multifunctional carboxyphenylphosphonate ligand derivatives.[5] Recent studies of uranyl phosphonates have shown promising applications in ionic conductivity, ion-exchange, intercalation chemistry, photochemistry, catalysis, and gas sorption.[3a,4a,b,6]

Inspired by earlier results and based on our previous work on coordination chemistry of actinide phosphonates, we are investigating the structural chemistry of uranium(VI) with arsonates. There is a dearth of knowledge concerning the solid-state chemistry and physical properties of uranyl arsonates. Some of the challenges facing the development of the structure−property relationships for actinide arsonates may be similar to difficulties associated with the structure chemistry of uranyl phosphonates. These are highly insoluble in water, organic solvents, and even in strongly acidic solutions.[7] They tend to precipitate as poorly ordered structures or amorphous powders, making it difficult to obtain a suitable crystal for single crystal X-ray determination.[7] Some of the earlier crystal

Received: September 5, 2012
Published: October 25, 2012

   dx.doi.org/10.1021/ic301942t | *Inorg. Chem.* 2012, 51, 12032−12040

structures were determined using ab initio powder diffraction methods.[3c,8]

The structural chemistry of metal arsonates are expected to be similar to those of the metal phosphonates, but the larger ionic radius and longer As−O bond length of As(V) compared to P(V) could greatly influence their structural and physical properties.[9a,b] Until the recently reported role of arsonates in preparation of uranyl complexes with cation−cation interactions, reports of metal arsonates were mostly limited to transition metals.[9b,c,10] The condensation of the arsonate ligand is conceivably the most intriguing, where the resulting pyroarsonate ligands (mostly produced in situ) coordinate with the metal ions to yield unusual structure architectures.[10] The condensation of phosphonate ligands have also been reported in a few metal phosphonate systems.[11] Herein we report the synthesis, structural characterization, and spectroscopic properties of a series of uranyl arsonates, $UO_2(C_6H_5)_2As_2O_5(H_2O)$ (**UPhAs-1**), $UO_2(HO_3AsC_6H_4AsO_3H)(H_2O)\cdot H_2O$ (**UPhAs-2**), and $UO_2(HO_3AsC_6H_4NH_2)_2\cdot H_2O$ (**UPhAs-3**).

EXPERIMENTAL SECTION

Synthesis. UO_3 (98% Strem), HF (48 wt %, Aldrich), phenylarsonic acid (Alfa Aesar, 97%), 1,2-phenylenediarsonic acid (Aldrich), and 4-aminophenylarsonic acid (98%, Aldrich) were used as received. Reactions were conducted in PTFE-lined Parr 4749 autoclaves with a 23 mL internal volume. Distilled and Millipore filtered water with a resistance of 18.2 MΩ·cm was used in all reactions.

Caution! *While the uranium used in these studies was isotopically depleted, precautions are needed for handling radioactive materials, and all studies should be conducted in a laboratory dedicated to studies of radioactive materials.*

$UO_2(C_6H_5)_2As_2O_5(H_2O)$ (UPhAs-1) and $UO_2(HO_3AsC_6H_4AsO_3H)(H_2O)\cdot H_2O$ (UPhAs-2). UO_3 (28.6 mg, 0.1 mmol), phenylarsonic acid (40.4 mg, 0.2 mmol), or 1,2-phenylenediarsonic acid (67.9 mg, 0.2 mmol), 0.5 mL of water, and HF (∼5 μL, 0.1 mmol) were loaded into a 23 mL autoclave. The autoclave was sealed and heated to 110−160 °C in a box furnace for 3−5 days and was then cooled at an average rate of 9 °C/h to 25 °C. The resulting yellow product was washed with distilled water and methanol, and allowed to dry in air. Yellow tablets or platelets of products of **UPhAs-1** or **UPhAs-2**, respectively, suitable for X-ray diffraction studies, were formed (yields: **UPhAs-1** = 71% and **UPhAs-2** = 68%, on the basis of uranium). No impurities were detected in the powder X-ray diffraction patterns for **UPhAs-1**, but the pattern corresponding to **UPhAs-2** contains a low-intensity peak at ∼12° 2θ that reveals the presence of an impurity phase that corresponds to less than 5% of the product.

$UO_2(HO_3AsC_6H_4NH_2)_2\cdot H_2O$ (UPhAs-3). UO_3 (28.6 mg, 0.1 mmol), 4-aminophenylarsonic acid (43.4 mg, 0.2 mmol), 0.5 mL of water, 0.2 mL of methanol, and HF (∼5 μL, 0.1 mmol) were loaded into a 23 mL autoclave. The autoclave was sealed and heated to 80−110 °C in a box furnace for 5 days and was then cooled at an average rate of 9 °C/h to 25 °C. The product was washed with distilled water and methanol. After drying, yellow needle-like crystals of **UPhAs-3** were isolated as a pure product (yield: 61% on the basis of uranium).

Crystallographic Studies. A single crystal of each of the compounds **UPhAs-1**, **UPhAs-2**, and **UPhAs-3** was mounted on a cryoloop and optically aligned on a Bruker APEXII Quazar CCD X-ray diffractometer using a digital camera. Initial intensity measurements were performed using a IμS X-ray source and a 30 W microfocused sealed tube (Mo Kα, λ = 0.71073 Å) with a monocapillary collimator. The APEXII software was used for determination of the unit cells and data collection control. The intensities of reflections of a sphere were collected by a combination of four sets of exposures (frames). Each set had a different φ angle for the crystal and each exposure covered a range of 0.5° in ω. A total of 1464 frames was collected with an exposure time per frame of 10−30 s, depending on the crystal size and quality. SAINT software was used for data integration including Lorentz and polarization corrections. Semiempirical absorption corrections were applied using the program SADABS. The program suite SHELXTL was used for space group determination (XPREP), direct methods structure solution (XS), and least-squares refinement (XL).[12] The positions of H atoms around the carbon atoms were included using a riding model. The final refinement included anisotropic displacement parameters for all atoms except H. Selected crystallographic information is listed in Table 1 and Supporting Information, Tables 2−4. Atomic coordinates, bond distances, and additional structural information are provided in the Supporting Information.

Table 1. Crystallographic Data for $UO_2(C_6H_5)_2As_2O_5(H_2O)$ (UPhAs-1), $UO_2(HO_3AsC_6H_4AsO_3H)(H_2O)\cdot H_2O$ (UPhAs-2), and $UO_2(HO_3AsC_6H_4NH_2)_2\cdot H_2O$ (UPhAs-3)

	UPhAs-1	UPhAs-2	UPhAs-3
formula mass	672.09	637.98	716.11
color and habit	yellow, tablet	yellow, platelet	yellow, needle-like
space group	$P2_1/c$ (No. 14)	$P\bar{1}$ (No. 2)	$C2/c$ (No. 15)
a (Å)	17.917(8)	8.0383(13)	23.999(5)
b (Å)	7.018(3)	12.336(2)	5.2714(12)
c (Å)	12.667(6)	15.889(3)	16.905(4)
α (deg)	90	77.787(2)	90
β (deg)	103.727(5)	81.552(2)	129.179(2)
γ (deg)	90	89.978(2)	90
V (Å)	1547.2(12)	1522.4(4)	1657.8(6)
Z	4	2	4
T (K)	100	100	100
λ (Å)	0.71073	0.71073	0.71073
ρ_{calcd} (g cm^{-3})	2.885	2.722	2.867
μ (Mo Kα) (mm^{-1})	14.773	15.012	13.806
$R(F)$ for $F_o^2 > 2\sigma(F_o^2)^a$	0.022	0.041	0.029
$Rw(F_o^2)^b$	0.045	0.118	0.074

$^a R(F) = \sum||F_o| - |F_c||/\sum|F_o|$. $^b R(F_o^2) = [\sum w(F_o^2 - F_c^2)^2/\sum w(F_o^4)]^{1/2}$.

Powder X-ray Diffraction (XRD). A powder XRD pattern for each compound was collected on a Bruker θ−θ diffractometer equipped with a Lynxeye one-dimensional solid state detector and Cu Kα radiation at room temperature over the angular range from 5° to 60° (2θ) with a scanning step width of 0.02° and a fixed counting time of 1 s/step. To determine the purity of the compounds, the experimental powder patterns were compared with the simulated powder patterns from single-crystal data of **UPhAs-1**, **UPhAs-2**, and **UPhAs-3** (see Supporting Information, Figures S1−S3).

Spectroscopic Properties. Absorption and fluorescence data were acquired from a single crystal of each of the compounds using a Craic Technologies UV−vis−NIR microspectrophotometer with a fluorescence attachment. The absorption data were collected in the range of 250−1200 nm at room temperature (see Supporting Information, Figure S5). Excitation was achieved using 365 nm light from a mercury lamp for the fluorescence spectroscopy. Raman spectra were collected for all the uranyl arsonate compounds using a Bruker Sentinel system linked via fiber optics to a video-assisted Raman probe in a microscope mount. The laser wavelength was 785 nm with a power of 400 mW. The instrument is equipped with a high-sensitivity, TE-cooled 1024 × 255 CCD array. Infrared spectra were collected from a single crystal of **UPhAs-1**, **UPhAs-2**, and **UPhAs-3** using a SensIR Technology IlluminatIR FT-IR microspectrometer. A single crystal of each compound was placed on a glass slide, and the spectrum was collected with a diamond ATR objective.

Thermogravimetric Analysis (TGA). TGA measurements were conducted for the three compounds using a Netzsch TG209 F1 Iris thermal analyzer for 10−15 mg of each sample in an Al_2O_3 crucible

dx.doi.org/10.1021/ic301942t | Inorg. Chem. 2012, 51, 12032−12040

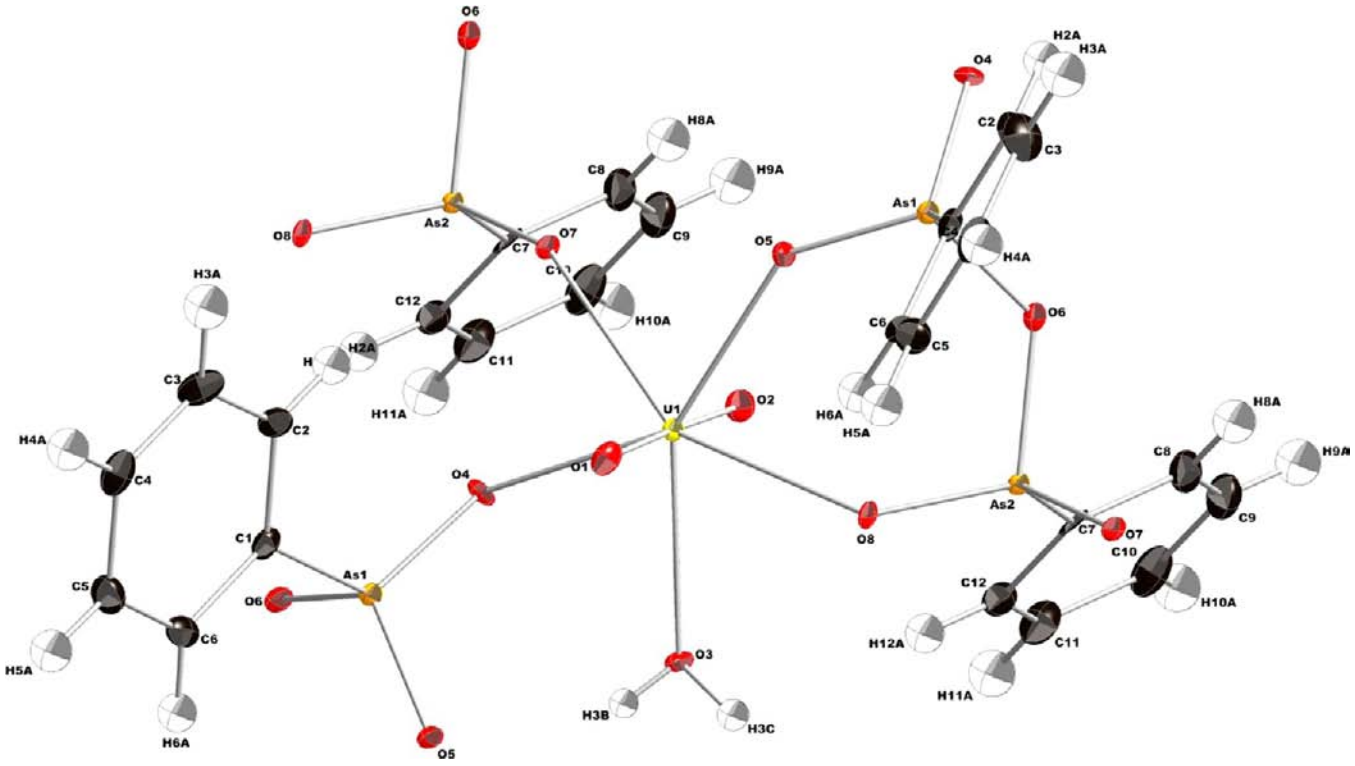

Figure 1. Representation of the local coordination environment in **UPhAs-1**. Ellipsoids are shown in the 50% probability level.

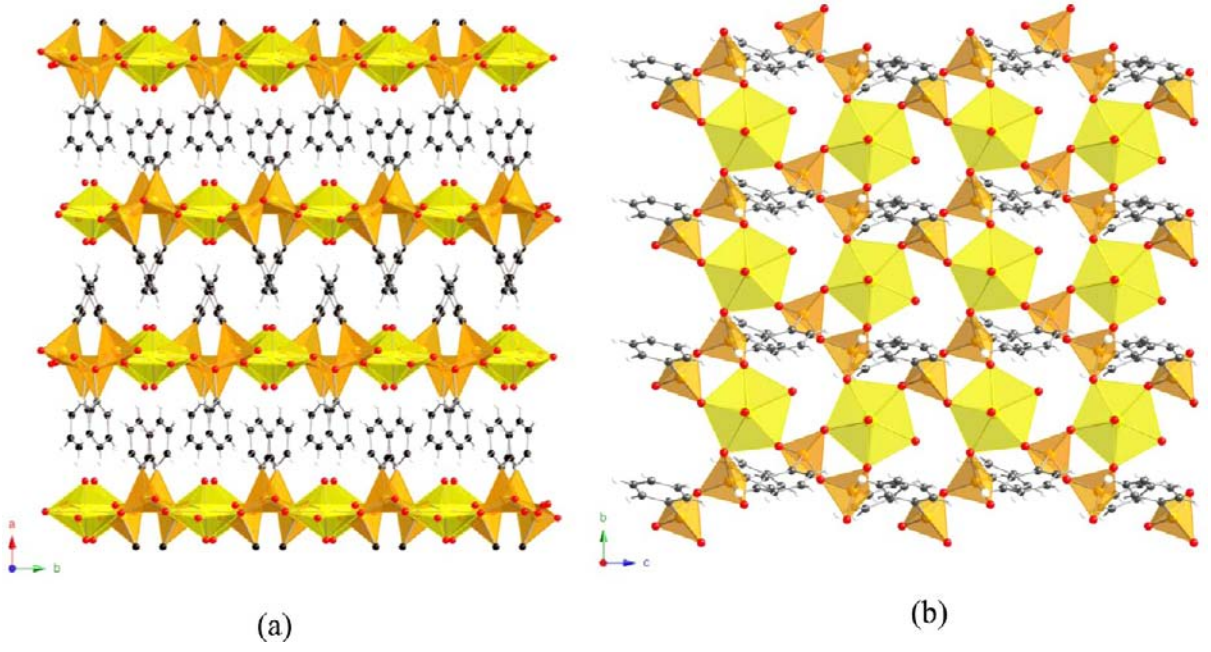

Figure 2. (a) Illustration of the layered structure of **UPhAs-1** as viewed along the *c-axis*. (b) Arrangement of the uranyl-pyroarsonate sheet structure in **UPhAs-1**. UO_7 units = yellow, arsenate = orange, oxygen = red, phenyl = carbon, hydrogen = white.

that was heated from 25 to 900 °C at a rate of 5 °C/min under flowing nitrogen gas.

RESULTS AND DISCUSSION

Synthesis. The stoichiometric ratio of 1:2 (U:As) was used in all of the syntheses reported here. The addition of HF to the reactants is essential; it serves as a mineralizing agent in all the syntheses. **UPhAs-1** and **UPhAs-2** can be prepared over a wide temperature range from 110 to 160 °C. **UPhAs-3** was synthesized over the temperature range of 80−110 °C; the ligand, 4-aminophenylarsonic acid, decomposes at higher temperature. Within the ranges specified here the product yields were constant.

Structure of $UO_2(C_6H_5)_2As_2O_5(H_2O)$ (UPhAs-1). The structure of **UPhAs-1** consists of a remarkable two-dimensional layered structure formed from a crystallographically distinct uranyl center that occurs in pentagonal bipyramids with a metal to pyroarsonate ratio of 1:1 (Figures 1 and 2). Phenylarsonic

dx.doi.org/10.1021/ic301942t | *Inorg. Chem.* 2012, 51, 12032−12040

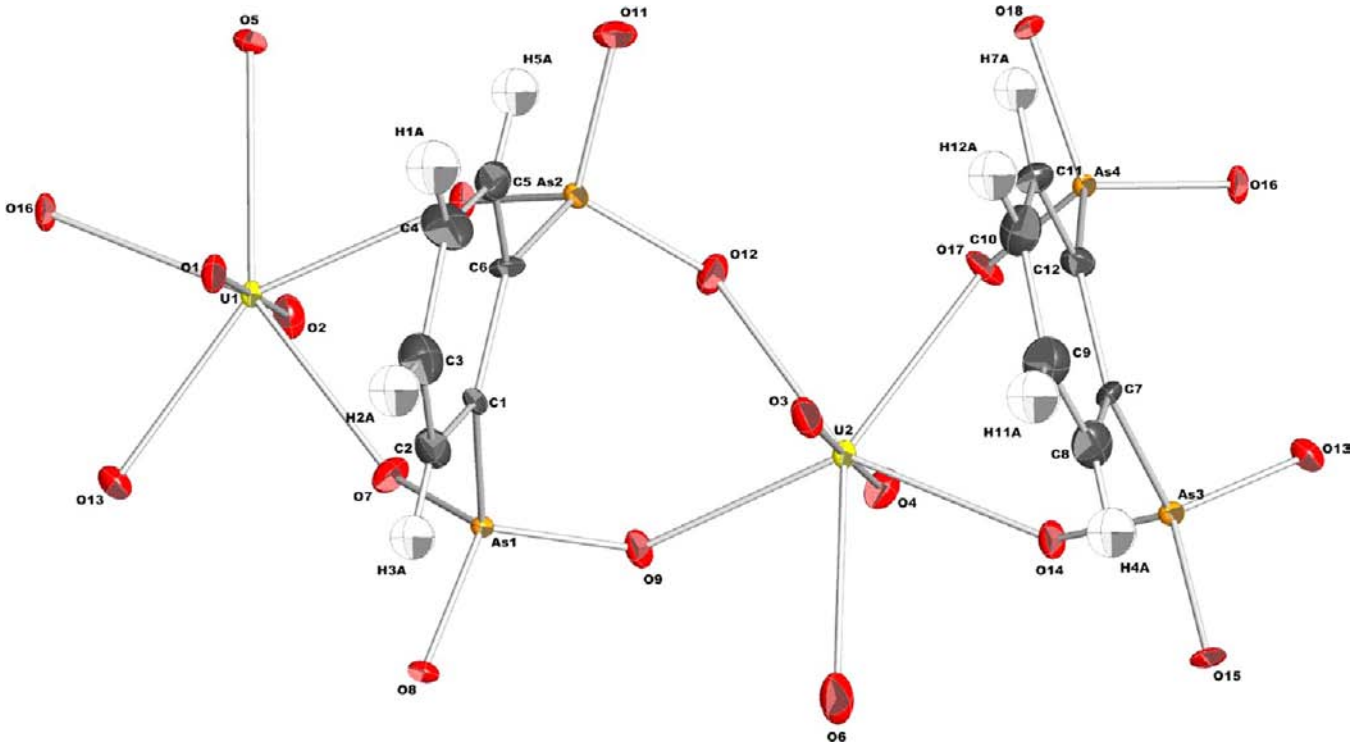

Figure 3. Depiction of the local coordination environment in **UPhAs-2**. Ellipsoids are shown in the 50% probability level.

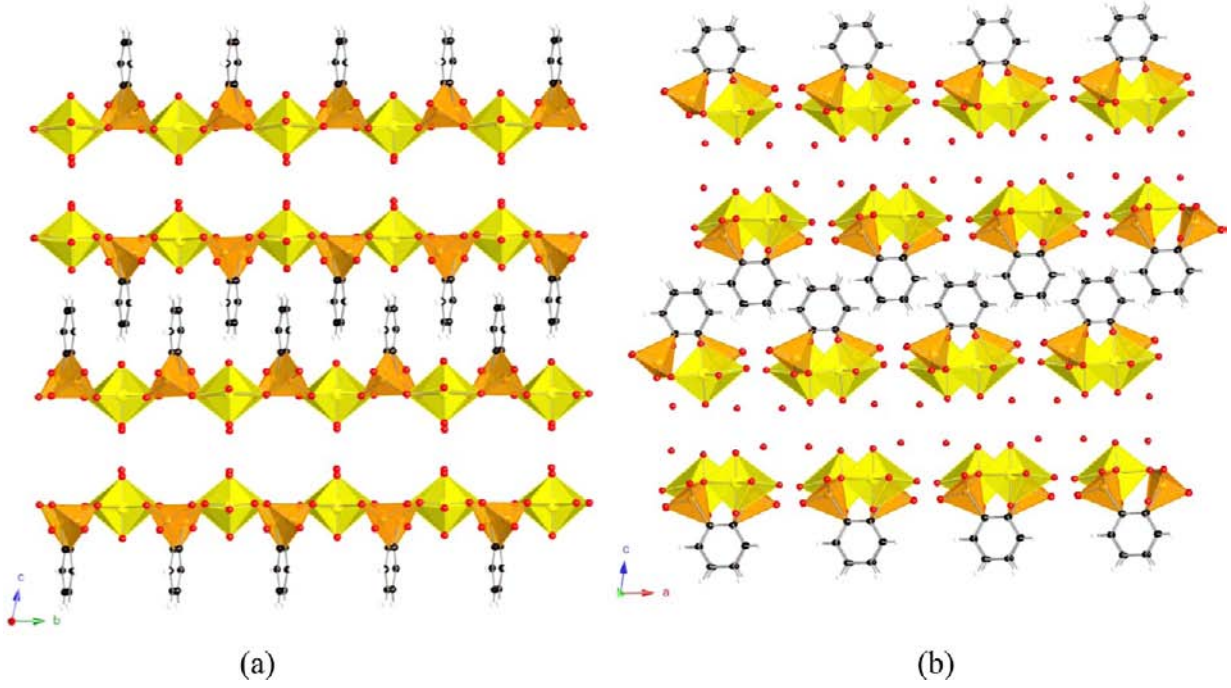

Figure 4. Two different views of the uranyl-phenylenediarsonate polyhedra found in **UPhAs-2**. UO_7 units = yellow, arsenate = orange, oxygen = red, phenyl = carbon, hydrogen = white.

acid units condensed in situ to form the fused tetrahedra of the pyroarsonate moiety, $PhAs(O_2)OAs(O_2)Ph]^{2-}$. Each uranyl cation is chelated by four oxygen atoms, in the equatorial plane of a bipyramid, that are from three different pyroarsonate moieties The fifth equatorial ligand of the pentagonal bipyramid is an oxygen atom of a water molecule. The phenyl groups of the same pyroarsonate moiety point in opposite directions and are intertwined with phenyl rings from another row. This can be ascribed to the steric influence of the bulky phenyl group. There are several reports concerning U(VI) complexes with phenylphosphonic acid, $PhPO_3H_2$ (pK_a = 1.86, 7.51), a well studied phosphonate ligand with similar organic residue as the phenylarsonic acid, $PhAsO_3H_2$ (pK_a = 3.39, 8.25).[13a] Most of the structures show the prevalence of one-dimensional linear chains of uranyl phenylphosphonates that are unlike the layered structure presented here (Figure 2).[3a,b] In

dx.doi.org/10.1021/ic301942t | *Inorg. Chem.* 2012, 51, 12032−12040

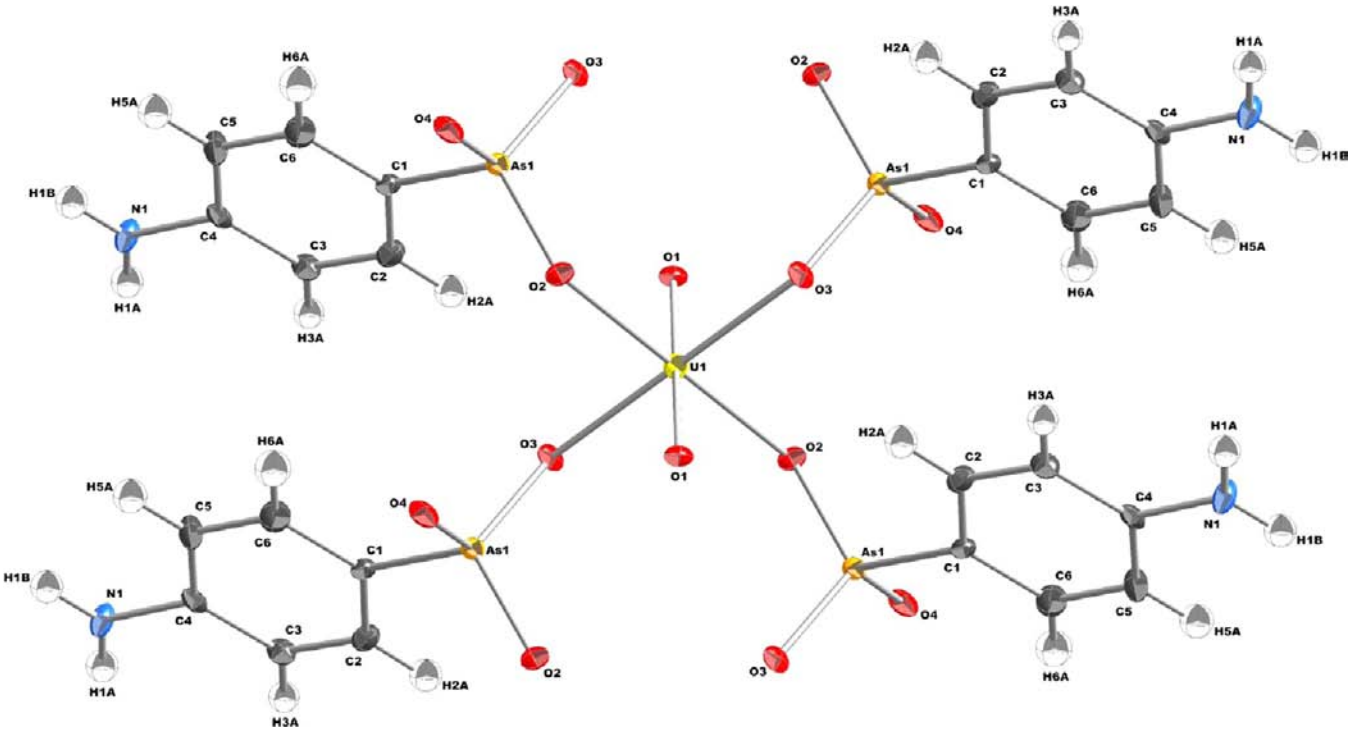

Figure 5. Drawing of the local coordination environment in **UPhAs-3**. Ellipsoids are shown in the 50% probability level.

contrast to **UPhAs-1**, most of the uranyl phenylphosphonate compounds are unstable in air or aqueous solution. Crystals of **UPhAs-1** were soaked in water or aqueous solution and were filtered after a week to examine their stability in water; the crystals were characterized using single-crystal and powder X-ray diffraction, and the results demonstrate that crystallinity is maintained. This preliminary study provides a clear indication of two neighboring pnictogens displaying very different physical and chemical behaviors.

It has been demonstrated that phenylarsonic acid can eliminate water to form As−O—As linkages via a metal-mediated, thermally induced condensation process.[10,13b] The preparation of **UPhAs-1** is also remarkable, in that all the reported pyroarsonate and pyrophosphonate compounds were prepared in acetonitrile under solvothermal conditions,[10,11b−e] with the only exception, $[Mo_2(OH)_2Cl_4(MeC_6H_4CH_3)PO(OEt)(O)O_2P(CH_2C_6H_4Me)]$, prepared in dichloromethane.[11a] A recently proposed mechanism for a series of Ag(I) pyrophosphonates by Zheng and co-workers illustrated the significance of C−C bond cleavage of the acetonitrile in the condensation reactions.[11d,e] To the best of our knowledge, there is no other reported example of uranyl-mediated condensation reactions in arsonate and phosphonate systems.

The uranium center is characteristically bound to two "yl" oxo atoms to form a nearly linear UO_2^{2+} cation, with an average U═O bond distance of 1.771(3) Å. The four oxygen atoms from the pyroarsonate ligand are bound to the uranyl center in the equatorial plane of the pentagonal bipyramid with U−O bond distances ranging from 2.357(3) to 2.385(3) Å. Two of these atoms are from chelating pyroarsonate ligands, and the remaining are from two independent arsonate ligands. The U−O(3) bond distance is 2.502(3) Å; this is the longest U−$O_{equatorial}$ bond length, and it is within the range expected for a coordinated water molecule.[5c] The calculated bond-valence sum for the uranyl cation is 6.02, consistent with the formal valence of U(VI).[14] The As−O bond lengths range from 1.655(3) to 1.785(3) Å, noticeably longer than P−O bond lengths.[3] All available oxygen atoms of the pyroarsonate moiety are involved in coordination to the uranyl cation. The O(6) atom bridges the two phenylarsonate groups, and represents the longest As−O bond length [1.785(3) Å].

Structure of $UO_2(HO_3AsC_6H_4AsO_3H)(H_2O)\cdot H_2O$ (UPhAs-2). **UPhAs-2** contains two crystallographically distinct U(VI) pentagonal bipyramids that are connected to each other through two AsO_3 groups from the same phenylenediarsonate ligand, with a metal to arsonate ligand ratio of 1:1 (see Figure 3). Each of the ligands chelates two adjacent uranyl cations to extend the chain into a one-dimensional structure (Figure 4). This structure is isotypic with a recently published Pu(VI) phosphonate.[15] The two phenyl rows are directed into the same area of the chain, creating both hydrophobic and hydrophilic regions, similar to α-UPP.[3a,b] The chains and arrangement of the phenyl rings are shown in Figure 4a-b. The hydrophilic region is filled with lattice water molecules, and their positions are disordered as reflected by relatively high displacement parameters. There is a solvent accessible void volume of 121 $Å^3$ containing 122 electrons count per cell as determined by PLATON/Squeeze.

Each uranium center is coordinated to two "yl" oxo atoms with U═O bond lengths that range from 1.774(7) to 1.793(7) Å. Owing to actinide contraction, these bond distances are longer than those observed in the Pu(VI) phosphonate complex.[15] An additional five oxygen atoms coordinate the uranium cation in the equatorial plane. Four of these are from phenylenediarsonate ligands, with U−O bond distances ranging from 2.319(6) to 2.364(6) Å. The longest U−O bond distances, 2.551(6) and 2.553(7) Å, are within the range for coordinated water molecules.[5c] The calculated bond-valence sums for the uranium centers are 6.04 and 6.01, consistent with the expected formal valence of U(VI).[14] Each of the uranium

dx.doi.org/10.1021/ic301942t | *Inorg. Chem.* 2012, 51, 12032−12040

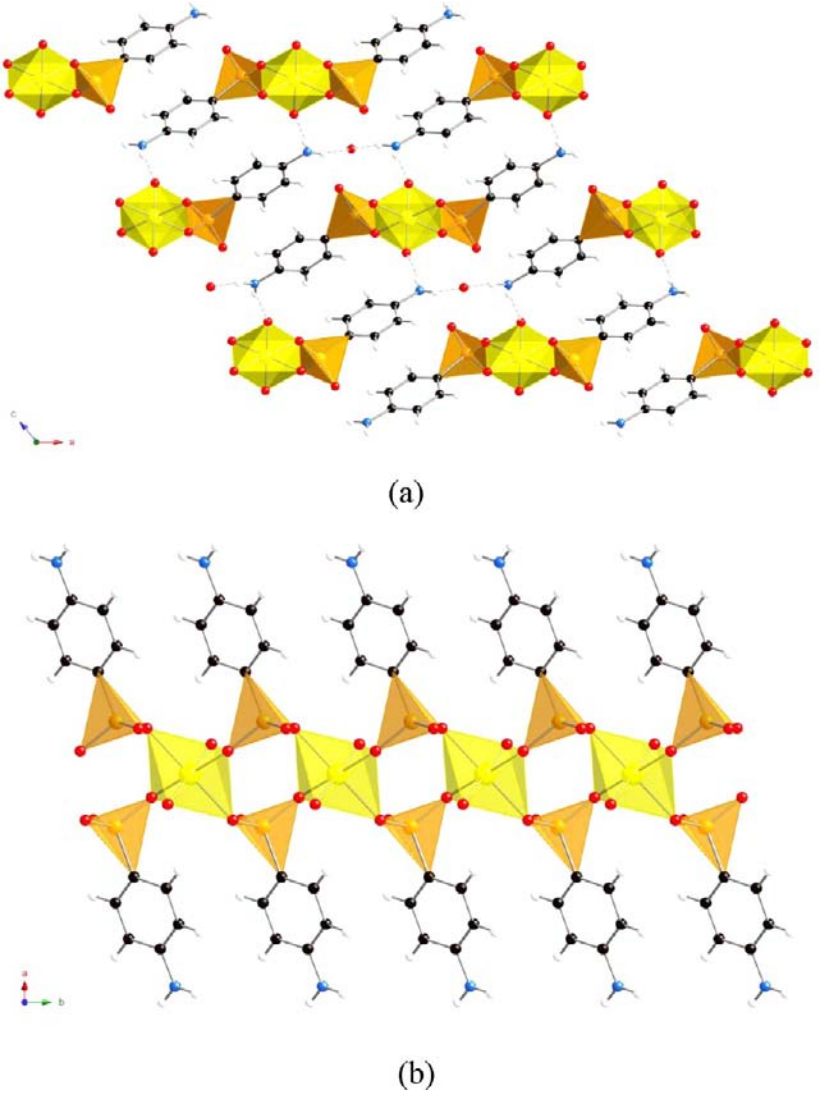

Figure 6. (a) View of **UPhAs-3** with projection of linear chains along the *b-axis*. The phenyl rings are stacked on each other in two rows in a trans fashion. (b) Illustration of **UPhAs-3** depicting the structure of one of the linear chains. UO_6 units = yellow, arsenate = orange, oxygen = red, nitrogen = blue, phenyl = carbon, hydrogen = white.

centers is chelated by two crystallographically distinct phenylenediarsonate ligands. The As−O bond distances are much longer than P−O bond distances, as they range from 1.669(6) to 1.705(6) Å.[15] In contrast to **UPhAs-1**, only two oxygen atoms of each arsonate moiety are used for chelating the uranyl cation; the third oxygen atoms [O(8), O(11), O(15), and O(18)] are the longest As−O bonds, as they are protonated and also correspond to terminal oxygen atoms from the arsonate groups.

Structure of $UO_2(HO_3AsC_6H_4NH_2)_2{\cdot}H_2O$ (UPhAs-3). **UPhAs-3** contains a crystallographically distinct U(VI) cation that is six-coordinate and that resides on a center of symmetry between the two pairs of adjacent arsonate ligands, with a metal to arsonate ratio 1:2 (Figure 5). The uranium geometry is a rare UO_6 tetragonally distorted octahedron (D_{4h}). As in **UPhAs-2,** it forms one-dimensional linear chains along the *b*-axis (see Figure 6). The two aniline rows point in opposite directions to give both sides of the chain a similar nature. The cocrystallized water molecule is hydrogen bonded to the -NH_2 groups. This structural topology is similar to that of $UO_2(HO_3PC_6H_5)_2{\cdot}2CH_3CH_2OH$, which is unstable at room temperature.[3b]

The U(VI) cation is coordinated to two centrosymmetrically related "yl" oxo atoms O(1) and O(1i) in the axial plane with a U═O bond distance of 1.818(5) Å. The U═O bond distance observed here is noticeably longer than those of the first two compounds described herein, a direct result of the different coordination environments. The $[O{=}U{=}O]^{2+}$ bond angle is 180.0(3)°, whereas the O−U—O bond angles in the equatorial plane are close to 90° (within 0.8). Two pairs of centrosymmetrically related oxygen atoms, O(2) and O(3ii), are arranged in the equatorial plane with U−O bond distances of 2.295(4) and 2.444(4) Å, respectively. Using these bond distances, we arrived at a bond-valence sum of 5.99 for U(1), which agrees with the assigned oxidation state of U(VI).[14] Two oxygen atoms of the arsonate group are used for binding the uranyl cation; the third oxygen atom is terminal, and it is protonated as in **UPhAs-2**. The As−O bond distances range from 1.671(5) to 1.681(4) Å and are longer than P−O bond distances.[3] Interactions of the $-NH_2$ group with the water and O_{axial} atom

dx.doi.org/10.1021/ic301942t | *Inorg. Chem.* 2012, 51, 12032−12040

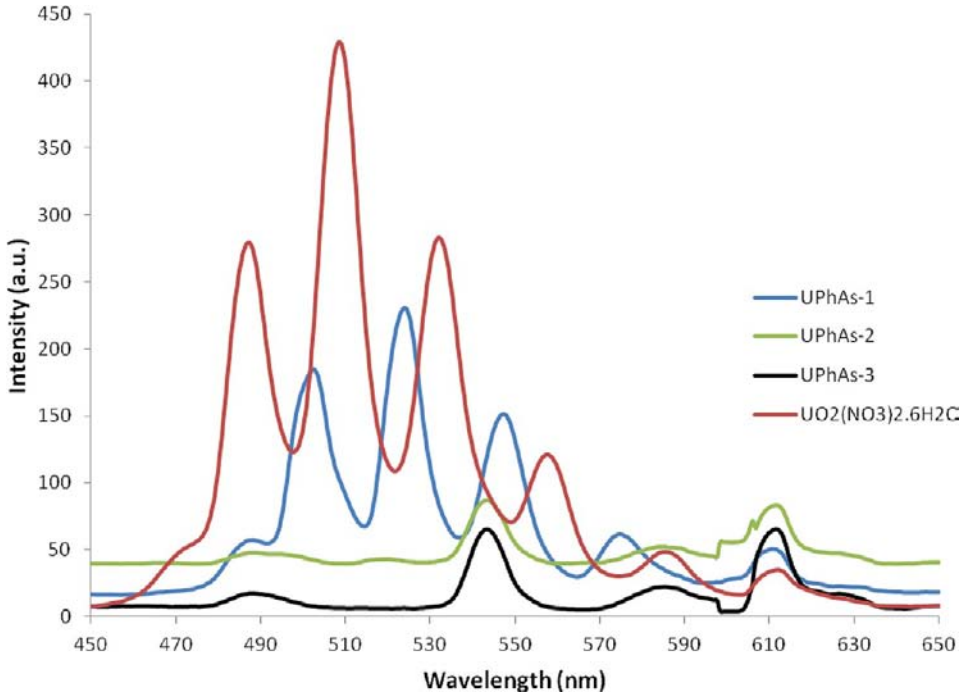

Figure 7. Fluorescence spectra of three uranyl arsonates and uranyl nitrate hexahydrate showing clearly resolved vibronically coupled charge-transfer transitions.

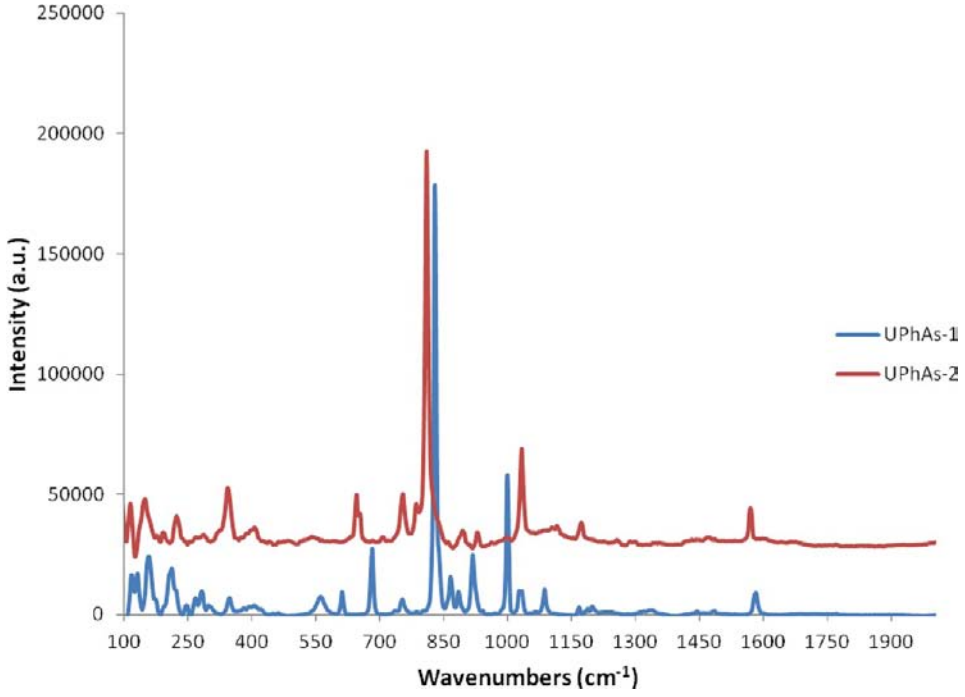

Figure 8. Raman spectra of **UPhAs-1** and **UPhAs-2**.

result in relatively strong hydrogen bonds, N−H···O (2.881−3.041 Å) that constitute the interlayer.

Spectroscopic Properties. UV−vis−NIR absorption spectroscopy has provided a useful diagnostic tool for characterizing uranium compounds in their various oxidation states (4+, 5+, and 6+). The absorption spectra for all three compounds are shown in Supporting Information, Figure S5. They reveal the characteristic equatorial U−O charge transfer bands of uranyl centered at 330 nm, and the axial U═O charge transfer bands are observed around 430 nm with characteristic vibronic fine-structure for U(VI).

Most uranyl containing compounds emit green light centered near 520 nm with strong vibronic coupling, yielding a well resolved five-peak pattern at room temperature.[16] However, not all compounds containing uranyl cations fluoresce and the mechanisms of the emission are often difficult to explain.[16] In contrast, Th(IV) has a $5f^0$ configuration and emissions are not expected, but we have observed luminescent properties in $ThF_2(PO_3C_6H_4CO_2H)$.[5h] The fluorescence spectra for the

dx.doi.org/10.1021/ic301942t | *Inorg. Chem.* 2012, 51, 12032−12040

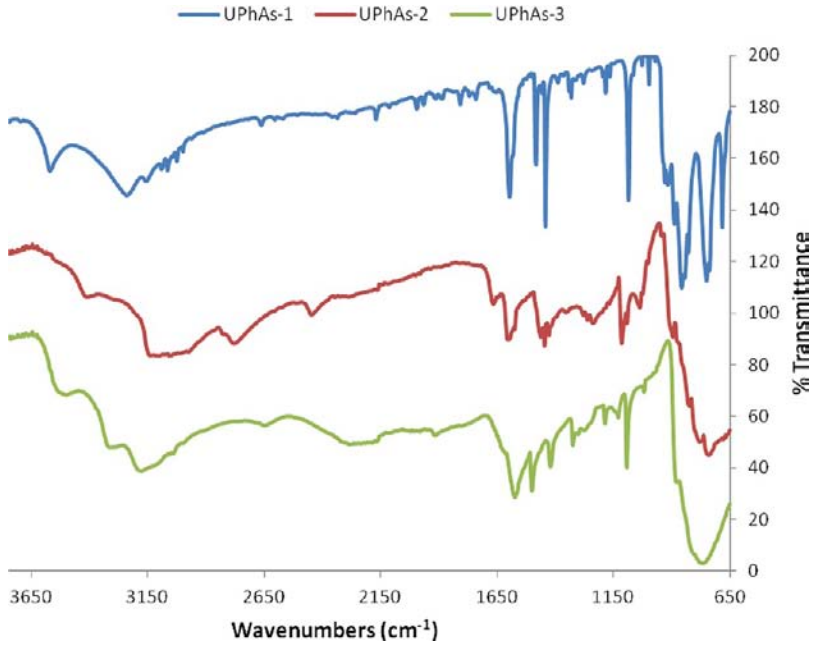

Figure 9. Infrared spectra of three uranyl arsonates.

three compounds were excited at 365 nm, and they reveal the emission pattern for uranyl compounds. **UPhAs-1** and **UPhAs-2** reveal the characteristic five-peak emission bands positioned at 503, 525, 547, 575, and 611 nm for **UPhAs-1** and are clearly resolved at 488, 520, 543, 585, and 611 nm for **UPhAs-2** (Figure 7). Only four peaks are clearly resolved for **UPhAs-3** at 488, 543, 585, and 611 nm. These compounds are red-shifted by approximately 16 nm (**UPhAs-1**) and 34 nm (**UPhAs-2** and **UPhAs-3**) relative to the corresponding five-band emission pattern in the spectrum of $UO_2(NO_3)_2{\cdot}6H_2O$. The slight differences can be ascribed to the influence of the arsonate ligands.

Raman spectra of **UPhAs-1** and **UPhAs-2** are shown in Figure 8, whereas **UPhAs-3** was not characterized because of poor Raman activity. The O−H bending vibrations of bound hydroxyl groups from lattice water and U-coordinated water molecules are observed at 1581 and 1568 cm^{-1} for **UPhAs-1** and **UPhAs-2**, respectively. The group of peaks between 1000 and 1086 cm^{-1} in **UPhAs-1**, and a sharper peak positioned at 1033 cm^{-1} in **UPhAs-2**, correspond to the As−O stretching mode of the arsonate groups. The band in the spectra at 914 cm^{-1} for **UPhAs-1** could be attributed to the ν (As−O−As), characteristic of pyroarsenate groups, while the band at 929 cm^{-1} for **UPhAs-2** would be attributed to the ν (As−C−C−As). The weak Raman bands around 885 cm^{-1} and 866 cm^{-1} can be attributed to stretching vibrations of (AsO_3Ph) and (As_2O_5). The most intense Raman bands at 830 for **UPhAs-1**, and 810 for **UPhAs-2**, are attributed to the uranyl group's symmetric stretch, ν_s (UO_2^{2+}). However, because of the overlap of peaks, definitive assignments are precluded in most cases at low wavenumber. The Raman band at 560 cm^{-1} in **UPhAs-1** is the symmetric bridge stretching vibration of the pyroarsonate group, ν_s (As−O—As). The 682 cm^{-1} peak in **UPhAs-1** or 645 cm^{-1} peak in **UPhAs-2** and bands at the low wavenumber regions are dominated by the phenyl ring, As−O group, and various lattice modes of the compounds.[5b,17]

The infrared spectra supplement the Raman spectra for **UPhAs-1** and **UPhAs-2**, and provide us with data for identifying the functional groups in **UPhAs-3**. The low wavenumber regions of the infrared spectra (Figure 9), 673−778 cm^{-1}, consist of peaks indicative of the phenyl ring stretching modes. IR peaks around 827−914 cm^{-1} in **UPhAs-1**, 824−895 cm^{-1} in **UPhAs-2**, and 876 cm^{-1} in **UPhAs-3** are attributed to stretching modes of the uranyl cation, UO_2^{2+}. Those bands at 1071−1091 cm^{-1}, 1037 cm^{-1}, and 1093 cm^{-1} are assigned to ν (As═O) stretches of **UPhAs-1**, **-2**, and **-3**, respectively. The C−H bending of the phenyl ring is positioned at 1443 cm^{-1} for **UPhAs-1**, 1445 cm^{-1} for **UPhAs-2**, and 1425 cm^{-1} for **UPhAs-3**. The broad band around 1600 cm^{-1} is indicative of H_2O bending. The high-energy regions are dominated by the O−H stretches of the lattice water and U-coordinated water. The peak at 3181 cm^{-1} is assigned to N−H stretches of the amine group in **UPhAs-3**, and the peak at 3586 cm^{-1} to O−H stretches of the uranyl coordinated water in **UPhAs-1**.[3b,4b,5d,f,i,17]

Thermogravimetric Analysis. The TGA curves for **UPhAs-1** indicate two main stages of weight losses (Supporting Information, Figure S6). The first weight loss begins at 150 °C and is complete by 248 °C, and is attributed to U-coordinated water molecules (∼2%). The second step occurs over the temperature range from 428 to 900 °C and corresponds to combustion of the ligand and the release of arsenic oxide (∼42%). **UPhAs-2** exhibits two distinct stages of weight losses. The first stage corresponds to the loss of lattice water molecules (∼3.5%), which occurs between 102 and 105 °C. The second broader weight loss occurs over the range of 248 to 900 °C, and is indicative of the loss of U-coordinated water molecules, combustion of the ligand, and the release of arsenic oxide (∼48.5%). The thermal stability curves for **UPhAs-3** show two distinct weight loses. The first is due to the loss of lattice water, beginning at 101 °C and ending at 105 °C (∼1%). The second weight loss occurs over a narrow temperature range that is followed by a broad tail in the range of 150 to 900 °C, and corresponds to the loss of U-coordinated water, combustion of the ligand, and the release of arsenic oxide (∼46.5%). The products resulting from the thermogravimetric

dx.doi.org/10.1021/ic301942t | *Inorg. Chem.* 2012, 51, 12032−12040

analyses of the three compounds were identified as UO_2 residues (see Supporting Information, Figure S4).

CONCLUSIONS

In this study, we selected some arylarsonic acids with similar organic components to previously studied arylphosphonic acids to correlate and contrast their coordination chemistry with uranium. This investigation has yielded several important observations and conclusions. Although As(V) shares the same group with P(V) on the periodic table, a relatively minor difference in ionic radius and bond length can produce dramatic structural differences as exemplified by **UPhAs-1**. First, the arsonate chemistry of uranium appears to be remarkably diverse, yielding the uranyl pyroarsonate complex that is without precedence. In addition, the arsonate group is more likely to be partially protonated (because of higher pK_a values), but **UPhAs-1** is completely deprotonated.[13a] In contrast to other reported pyroarsonates and pyrophosphonates that were prepared under solvothermal conditions,[10,11] **UPhAs-1** was prepared using hydrothermal conditions. This can be ascribed to the much different characteristic properties of actinides relative to other transition metals. Second, the structural topologies of **UPhAs-2** and **UPhAs-3** are similar to those of well-studied arylphosphonates, but their physicochemical properties differ. The three uranyl arylarsonate compounds prepared show interesting stability in air and water. Third, the arylarsonate ligands in **UPhAs-1** and **UPhAs-2** complexes are both chelating to the central uranyl cations, thus yielding highly stable uranyl products. These interesting physical and chemical phenomena provide for preparing uranyl arsonates with unusual structural architectures, and testing uranyl arsonates in a variety of other important applications in the future.

ASSOCIATED CONTENT

Supporting Information

Selected interatomic distances (Å) and angles, powder X-ray diffraction patterns, absorption spectra, TGA curves, and crystallographic data (CIF) of three uranyl arsonates. This material is available free of charge via the Internet at http://pubs.acs.org.

AUTHOR INFORMATION

Corresponding Author

*E-mail: pburns@nd.edu.

Notes

The authors declare no competing financial interest.

ACKNOWLEDGMENTS

This material is supported by the Chemical Sciences, Geosciences and Biosciences Division, Office of Basic Energy Sciences, Office of Science, U.S. Department of Energy, Grant DE-FG02-07ER15880.

REFERENCES

(1) (a) Nash, K. L. *J. Alloys Cmpd.* **1994**, *213-214*, 300. (b) Nash, K. L. *J. Alloys Cmpd.* **1997**, *249*, 33. (c) Jensen, M. P.; Beitz, J. V.; Rogers, R. D.; Nash, K. L. *J. Chem. Soc., Dalton Trans.* **2000**, *18*, 3058.

(2) Clearfield, A., Demadis, K., Eds.; *Metal Phosphonate Chemistry: From Synthesis to Applications*; The Royal Society of Chemistry: Cambridge, U.K., 2012.

(3) (a) Grohol, D.; Clearfield, A. *J. Am. Chem. Soc.* **1997**, *119*, 4662. (b) Grohol, D.; Subramanian, M. A.; Poojary, D. M.; Clearfield, A. *Inorg. Chem.* **1996**, *35*, 5264. (c) Grohol, D.; Clearfield, A. *J. Am. Chem. Soc.* **1997**, *119*, 9301.

(4) (a) Adelani, P. O.; Albrecht-Schmitt, T. E. *Angew. Chem., Int. Ed.* **2010**, *49*, 8909. (b) Adelani, P. O.; Albrecht-Schmitt, T. E. *Inorg. Chem.* **2011**, *50*, 12184.

(5) (a) Doran, M. B.; Norquist, A. J.; O'Hare, D. *Chem. Mater.* **2003**, *15*, 1449. (b) Adelani, P. O.; Albrecht-Schmitt, T. E. *Inorg. Chem.* **2009**, *48*, 2732. (c) Adelani, P. O.; Oliver, A. G.; Albrecht-Schmitt, T. E. *Cryst. Growth Des.* **2011**, *11*, 1966. (d) Adelani, P. O.; Albrecht-Schmitt, T. E. *Cryst. Growth Des.* **2011**, *11*, 4227. (e) Adelani, P. O.; Albrecht-Schmitt, T. E. *J. Solid State Chem.* **2012**, *192*, 377. (f) Adelani, P. O.; Albrecht-Schmitt, T. E. *Cryst. Growth Des.* **2011**, *11*, 4676. (g) Adelani, P. O.; Oliver, A. G.; Albrecht-Schmitt, T. E. *Cryst. Growth Des.* **2011**, *11*, 3072. (h) Adelani, P. O.; Albrecht-Schmitt, T. E. *Inorg. Chem.* **2010**, *49*, 5701. (i) Adelani, P. O.; Oliver, A. G.; Albrecht-Schmitt, T. E. *Inorg. Chem.* **2012**, *51*, 4885.

(6) (a) Clearfield, A. *Prog. Inorg. Chem.* **1998**, *47*, 371. (b) Cao, G.; Hong, H.-G.; Mallouk, T. E. *Acc. Chem. Res.* **1992**, *25*, 420. (c) Clearfield, A. *Curr. Opin. Solid State Mater. Sci.* **2003**, *6*, 495. (d) Mao, J.-G. *Coord. Chem. Rev.* **2007**, *251*, 1493. (e) Alsobrook, A. N.; Hauser, B. G.; Hupp, J. T.; Alekseev, E. V.; Depmeier, W.; Albrecht-Schmitt, T. E. *Chem. Commun.* **2010**, *46*, 9167.

(7) Gagnon, K. J.; Perry, H. P.; Clearfield, A. *Chem. Rev.* **2011**, *112*, 1034.

(8) (a) Aranda, M. A. G.; Cabeza, A.; Bruque, S.; Poojary, D. M.; Clearfield, A. *Inorg. Chem.* **1998**, *37*, 1827. (b) Poojary, D. M.; Cabeza, A.; Aranda, M. A. G.; Bruque, S.; Clearfield, A. *Inorg. Chem.* **1996**, *35*, 1468. (c) Cabeza, A.; Aranda, M. A. G.; Cantero, F. M.; Lozano, D.; Martínez-Lara; Bruque, S. *J. Solid State Chem.* **1996**, *121*, 181. (d) Poojary, D. M.; Grohol, D.; Clearfield, A. *Angew. Chem., Int. Ed. Engl.* **1995**, *34*, 1508.

(9) (a) Mao, J. G. In *Metal Phosphonate Chemistry: From Synthesis to Applications*; Clearfield, A., Demadis, K., Eds.; The Royal Society of Chemistry: Cambridge, U.K., 2012; pp 133−169. (b) Tian, T.; Yang, W.; Pan, Q.; Sun, Z. *Inorg. Chem.* **2012**, *51* (20), 11150−11154. (c) Adelani, P. O.; Burns, P. C. *Inorg. Chem.* **2012**, *51* (20), 11177−11183.

(10) (a) Salta, J.; Chang, Y.; Zubieta, J. *J. Chem. Soc., Chem. Commun.* **1994**, 1039. (b) Mason, M. R.; Matthews, R. M.; Mashuta, M. S.; Richardson, J. F. *Inorg. Chem.* **1997**, *36*, 6476.

(11) (a) Chang, Y.; Zubieta, J. *Inorg. Chim. Acta* **1996**, *245*, 177. (b) Khan, M. I.; Zubieta, J. *Angew. Chem., Int. Ed. Engl.* **1994**, *33*, 760. (c) Yucesan, G.; Ouellette, W.; Golub, V.; O'Connor, C. J.; Zubieta, J. *Solid State Sci.* **2005**, *7*, 445. (d) Guo, L.; Bao, S.; Li, Y.; Zheng, L. *Chem. Commun.* **2009**, 2893. (e) Guo, L.; Tong, J.; Liang, X.; Kohler, J.; Nuss, J.; Li, Y.; Zheng, L. *Dalton Trans.* **2011**, *40*, 6392.

(12) Sheldrick, G. M. *Acta Crystallogr.* **2008**, *A64*, 211.

(13) (a) Yi, F.; Zhao, N.; Wu, W.; Mao, J. *Inorg. Chem.* **2009**, *48*, 628. (b) Doak, G. O.; Freedman, L. D. *Organometallic compounds of Arsenic, Antimony, and Bismuth*; John Wiley and Sons, Inc.: New York, 1970; p 45.

(14) (a) Burns, P. C.; Ewing, R. C.; Hawthorne, F. C. *Can. Mineral.* **1997**, *35*, 1551. (b) Brese, N. E.; O'Keeffe, M. *Acta Crystallogr.* **1991**, *B47*, 192.

(15) Diwu, J.; Wang, S.; Good, J. J.; DiStefano, V. H.; Albrecht-Schmitt, T. *Inorg. Chem.* **2011**, *50*, 4842.

(16) Liu, G.; Beitz, J. V. In *The Chemistry of the Actinide and Transactinides Elements*; Morss, L. R., Edelstein, N. M., Fuger, J., Eds.; Springer: Heidelberg, Germany, 2006; p 2088.

(17) (a) Kwak, W.; Rajkovic, L. M.; Stalick, J. K.; Pope, M. T.; Quicksall, C. O. *Inorg. Chem.* **1976**, *15*, 2778. (b) Mihajlovic, T.; Libowitzky, E.; Effenberger, H. *J. Solid State Chem.* **2004**, *177*, 3963. (c) Yi, F.; Song, J.; Zhao, N.; Mao, J. *J. Solid State Chem.* **2008**, *181*, 1393. (d) Cejka, J.; Sejkora, J.; Frost, R. L.; Keeffe, E. C. *J. Raman Spectrosc.* **2009**, *40*, 1521.